Talanta 115 (2013) 823–829

Contents lists available at SciVerse ScienceDirect

Talanta

journal homepage: www.elsevier.com/locate/talanta

Multifunctional phenylboronic acid-tagged fluorescent silica nanoparticles via thiol-ene click reaction for imaging sialic acid expressed on living cells ☆

Liwei Cheng, Xianxia Zhang, Zhengyong Zhang, Hui Chen, Song Zhang *, Jilie Kong *

Department of Chemistry, Fudan University, No. 220, Handan Road, Shanghai 200433, China

ARTICLE INFO

Article history:
Received 3 April 2013
Received in revised form
25 June 2013
Accepted 28 June 2013
Available online 4 July 2013

Keywords:
Living cell imaging
Sialic acid
Fluorescent silica nanoparticles
Phenylboronic acid tag
Thiol-ene click reaction

ABSTRACT

Multifunctional fluorescent silica nanoparticles with phenylboronic acid tags were developed for labeling sialic acid on the surface of living cancer cells. In this paper, fluorescent silica nanoparticles (FSNPs) with strong and stable emission at 515 nm were firstly prepared through a reverse microemulsion process, and then modified with highly selective phenylboronic acid (PBA) tags on their surface via an aqueous 'thiol-ene' click reaction. These nanoparticles had a hydrodynamic diameter of 92.6 ± 9.1 nm, and a bright fluorescence signal, which is 366 times higher than that of a single dye molecule. Meanwhile, these PBA-tagged FSNPs were found very stable in aqueous solution as well as in cell culture medium, verified by transmission electron microscopy, X-ray photoelectron spectroscopy and zeta potential analysis. The over-expressed sialic acid (SA) on the membrane of living HeLa cells was visualized in situ by a confocal laser scanning microscopy, ascribed to the specific interaction between PBA and SA. Thus, the PBA-FSBPs showed a great potential in probing SA expressed on living cells with high selectivity and sensitivity.

1. Introduction

Glycosylations, or the alternations of cell surface glycan structures, are dynamic and stage-specific processes during numerous normal and pathological processes including developments and differentiations [1,2]. Notably, most tumor-associated carbohydrate antigens are those clinically approved as tumor markers, which include sialic acid, an anionic monosaccharide that frequently occurs at the termini of the glycan chains. Indeed, increasing evidence has revealed that changes in sialic acid expression are closely associated with various disease states such as cancer, cardiovascular, and neurological diseases [3–5]. Furthermore, sialic acid is also used as a targeting moiety in an antitumor prodrug, owing to its binding ability to selectins that exist in the plasma membrane of cancer cells [6]. Although there are many methods, such as mass spectrometry and chromatography, for glycomic detection, they are not suitable for profiling glycan expression on living cell surface because of their destructivity. Therefore, with the goal for understanding the roles of sialic acid in disease development and providing diagnostic tools to guide treatment, it is necessary to develop a simple, sensitive and noninvasive method for labeling sialic acid on the surface of living cancer cells [7].

Developing the methodology in profiling glycan expression on cell surface with good selectivity and sensitivity is crucial for early diagnosis and also a great challenge for researchers. The common noninvasive strategy is based on the selective lectin–carbohydrate interaction on the surface of living cells, and some methods including patterning technology based on lectin-nanoparticle [8], lectin-array-based microscopic approaches [9–11] and probe-tagged lectin-based electrochemical strategies [12,13] have been developed. However, the applications of these lectin-based methods were limited by the relatively low affinities of lectins [14–17]. Notably, PBA, a synthetic molecule, has been demonstrated to make stable complexes with sugar containing 1,2- or 1,3-diol structures such as mannose and galactose at a pH higher than its pKa value of 8.63 [18,19]. Matsumoto et al. recently reported that SA can exceptionally form stable binding with undissociated PBA at physiological pH of 7.4 [20,21]. The anomalous complexing ability is correlated to the different binding modality of the PBA-SA complex from other sugars. This interesting finding provides an innovating molecular-targeting platform for labeling the expression of SA on living cells. Thus, Liu et al. reported a new quantum dot (QD)-based probe with small molecular PBA tags, which was applied to highly

* Corresponding authors.
E-mail addresses: Songzhang@fudan.edu.cn (S. Zhang), Jlkong@fudan.edu.cn (J. Kong).

0039-9140/$ - see front matter © 2013 Elsevier B.V. All rights reserved.
http://dx.doi.org/10.1016/j.talanta.2013.06.060

specific and efficient labeling sialic acids on living cells [22]. Han et al. reported the application of a double signal amplification strategy with glyconanoparticles and PBA-functionalized QD probes to improve the sensitivity for in situ monitoring SA on living cells [23]. The combination of QD with individual PBA ligands provides a good multifunctional cell-labeling probe for targeting specific SA with high sensitivity and selectivity, however, the inherently potential biotoxicity of QDs and the time-consuming multisteps will limit the application of those QD-based methods for in-vivo imaging of cancer cells. Notably, FSNPs also worked as a good cell-imaging material, but they have better biocompatibility and hydrophilicity, and easy surface modification than QDs [24–27]. Thus, we attempted to synthesize highly sensitive FSNPs with highly selective PBA tags for imaging sialic acid on living cells.

Herein, an effective "thiol-ene" chemistry reaction was used to covalently immobilize PBA tags on the surface of FSNPs. The thiol-ene click reaction offers all the advantages of click chemistry, but is simpler than those Cu-catalyzed azide-alkyne cycloadditions (CuAAC) and does not need copper-based toxic catalysts and easy-explosive azide chemicals [28]. As a promising metal-free reaction, the thiol-ene click reaction has an essentially outlook in biological modifications, such as "clicking" polymer brushes [29], surface glycosylation of polymer [30], and cell surface modification [31]. In this work, well-dispersed FSNPs were firstly synthesized by reverse microemulsion, and subsequently modified with PBA tags on the surface by a 'thiol-ene' click reaction (as shown in Fig. 1). HeLa (Human cervical carcinoma) cells were chosen as a model of cancer cell lines to demonstrate the specific recognition between PBA-FSNPs and SA, which have overproduction of SA groups [32]. The specificity of PBA-FSNPs for labeling of SA on living cells was investigated by flow cytometric analysis and confocal laser scanning microscopy.

2. Experimental

2.1. Reagents and materials

Fluorescein isothiocyanate (FITC), 3-aminopropyl trimethoxysilane (APTMS), paraformaldehyde, 3-(4,5-dimethylthiazol-2yl)-2,5-diphenyl-tetrazolium bromide (MTT), **SA** and 4-mercaptophenylboronic acid (MPBA) were obtained from Sigma-Aldrich Company (USA). Triethoxyvinylsilane (TEVS) was purchased from Aladdin Chemistry Co. Ltd. Benzophenone, mannose (Man), galactose (Gal) and glucose (Glu) were purchased from Sinopharm Chemical Reagant Co. Ltd. Tetraethyl orthosilicate (TEOS) and dimethylsulfoxide (DMSO) were bought from Shanghai Lingfeng Chemical Reagent Co. Ltd. (Shanghai, China). Triton X-100 was purchased from Alfa Aesar Co., Ltd. (Tianjing, China). 4, 6-Diamino-2-phenylindole (DAPI) was purchased from Key Gen Biotechnology Co. Ltd. (Nanjing, China). Fetal bovine serum (FBS), Dulbecco's modified eagle medium (DMEM), penicillin/streptomycin were purchased from Gibco (USA). All other reagents and solvents were of analytical grade and used as received. Doubly distilled water was used throughout.

2.2. Apparatus

UV–vis absorption spectra were recorded in a Shimadzu UV-3150 spectrophotometer. The size and morphology of FSNPs were characterized by transmission electron microscopy (TEM) using a JEOL model JEM-2011(HR) at 200 kV. Zeta potential measurements of FSNPs were carried out using a Malvern Zeta sizer (Nano series, Malvern Instruments Inc., USA). X-ray photoelectron spectroscopy (XPS) were carried out on a RBD upgraded PHI-5000C ESCA system (Perkin Elmer). Fluorescence spectra were recorded on a Cary Eclipse spectrophotometer (Agilent Co., U.S.A.) with an excitation wavelength at 488 nm. Flow cytometric analysis (FCA) was performed on a FACS Calibur flow cytometer (Becton Dickinson, U.S.A.). The fluorescence images of cells were recorded on a TCS SP5 confocal laser scanning microscopy (CLSM, Leica Co., Germany) with a Leica application suite, advanced fluorescence confocal scanning system.

2.3. Synthesis of FSNPs

The FSNPs were prepared by a reverse microemulsion including three processes (as shown in Fig. 1A), i.e. pre-modification of FITC with APTMS, subsequent hydrolysis and polymerization with TEOS, and surface vinyl-functionalization with TEVS. Firstly, fluorescent probes of FITC (2 mg) was covalently linked to APTMS

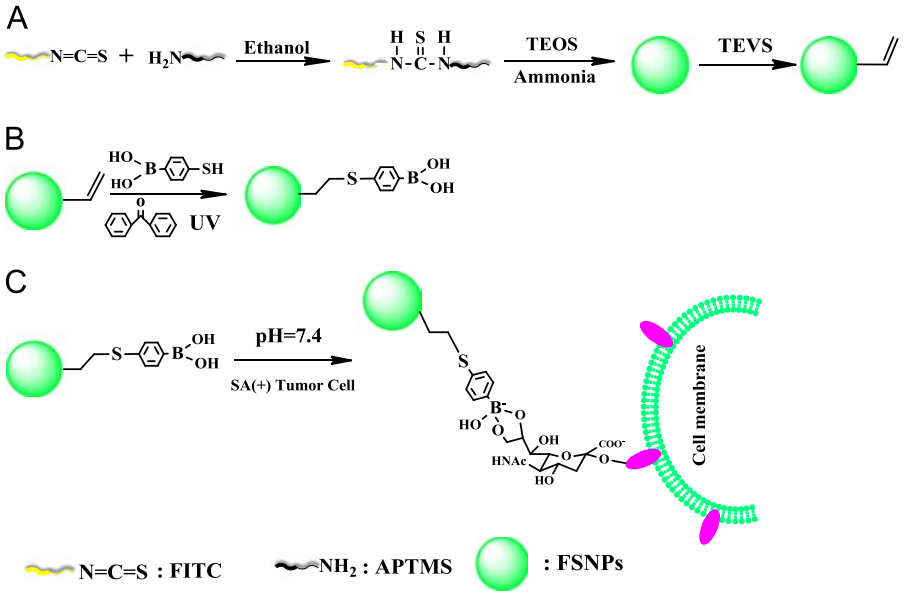

Fig. 1. Schematic illustration of the synthesis of multifunctional fluorescent probes, PBA-FSNPs, and their application for specific labeling of SA on living cancel cells. (A) The preparation of FSNPs by a reverse microemulsion, (B) the surface modification of FSNPs with PBA tags by a thiol-ene click reaction, and (C) specific labeling of PBA-FSNPs with SA on living cells.

(10 μL) by a dissolution in a molar ratio of 1:10, and then 2 mL ethanol was added in this solution and stirred for 24 h in dark prior to use. Secondly, a typical water-in-oil microemulsion solution was prepared by 7.5 mL of cyclohexane mixed with 1.77 mL of Triton X-100 and 1.80 mL of n-hexanol, and then 300 μL of water were added and stirred for 30 min at room temperature. Next, 50 μL of FITC/APTMS/ethanol solution were added dropwise to the microemulsion solution and stirred for 10 min. Subsequently, 100 μL of TEOS and 60 μL of aqueous ammonium hydroxide solution (25%) were added dropwise to the solution, respectively, and stirred for 24 h in the dark. Thirdly, in order to obtain the vinyl-functionalized nanocomposites, 50 μL of TEVS were added dropwise to the system. By continuing stirring for 19 h, the vinyl-functionalized FSNPs were obtained after adding 5 mL of acetone to break up the microemulsion. Finally, the resulting products of FSNPs (capped with vinyl) were centrifuged at 12,000 rpm and washed several times with ethanol and deionized water to remove the surfactant molecules and excess FITC molecules.

2.4. Synthesis of PBA-FSNPs

In attaching SA to living cells, PBA tags were initially conjugated to FSNPs using a 'thiol-ene' click reaction as shown in Fig. 1B. In this experiment, 4 mg/mL FSNPs with surface vinyls was mixed with MPBA (20 mM) and 1 wt% benzophenone in THF and H_2O (1:1 V/V), and subsequently initiated by the irradiation of UV light (λ_{max}=365 nm, 12 mW cm^{-2}) for 20 min. The PBA-FSNPs were collected by centrifugation at 12,000 rpm, and washed several times with ethanol and deionized water in order to remove the nonconjugated MPBA. The obtained PBA-FSNPs were kept at 4 °C prior to use.

2.5. Cell culture

HeLa cells and normal human astrocyte (NHA) cells were purchased from Cell Bank of Chinese Academy of Sciences. HeLa cells were cultured in DMEM media supplemented with 5% FBS and incubated at 37 °C in a humidified atmosphere containing 5% CO_2 in a Themo culturist. NHA cells were cultured in DMEM media supplemented with 10% FBS, 1% L-glutamine, 1% penicillin, and 1% streptomycin. The cell density was determined using a hemocytometer, and this was performed prior to any experiments.

2.6. Cytotoxicity assay

In vitro cytotoxicity of these multifunctional FSNPs was evaluated by performing MTT assays with HeLa cells. HeLa cells were seeded at 2×10^4 per cell into a 96-well culture plate in DMEM with 5% fetal bovine serum at 37 °C and with 5% CO_2 for 24 h. Next, the cells were incubated in different concentrations (50 μg/mL, 100 μg/mL, 500 μg/mL) of the PBA-FSNPs or FSNPs and without nanoparticles (as control experiments) for 24 h. Subsequently, 20 μL MTT (5 mg/mL) was added to each well of the plate and incubated for 4 h at 37 °C. The assays were performed according to the manufacturer's instructions. Next, the media containing MTT were replaced with 100 μL of DMSO to solubilize the precipitate of formazan crystals. Finally, the plate was shaken for 10 min at 37 °C before the measurement of optical absorbance at 492 nm by an automatic ELISA analyzer (SPR-960). All experiments were triplicated, and results were averaged.

2.7. Monosaccharide inhibition assays by FCA

Monosaccharide inhibition assays of PBA-FSNPs were performed by FCA to test their specific recognition for SA on the surface of cancer cells. Herein, PBA-FSNPs were replaced with inhibited PBA-FSNPs by pre-incubating with 5 mM Man, Gal, Glu, or SA for 1 h before incubation with HeLa cells (1×10^6 cells/mL). HeLa cells were cultured in 6-well plates for 12 h to preserve in their exponential growth phases, and collected by centrifugation at 1000 rpm for 6 min. The cell was washed for twice with PBS and resuspended in PBS, and this cell density was measured. Subsequently, HeLa cells (1×10^6 cells/mL) were incubated with four inhibited PBA-FSNPs (100 μg/mL) in 500 μL PBS for 20 min, respectively. These cells were collected by centrifugation at 1000 rpm for 6 min, washed twice with 400 μL of PBS, resuspended in 500 μL of PBS, and then measured by FCA. Notably, HeLa cells labeled with PBA-FSNPs were used as the control sample, and the fluorescence intensity of single labeled cell sample was calculated as the geometric mean by counting 10,000 events in FCA and deducted that of the autofluorescence of HeLa cells.

2.8. Cell fluorescence images by CLSM

The specificity of PBA-FSNPs for labeling of SA on living cells was investigated by CLSM. After HeLa cells were seeded on cover slips in DMEM with 5% FBS at 37 °C and with 5% CO_2 for 24 h, the medium was replaced with the reduced serum DMEM containing 100 μg/mL PBA-FSNPs. The cells were cultured for another 20 min at 37 °C and with 5% CO_2. Then, the cells were washed three times with PBS (pH 7.4) to remove the loosely attached nanoparticles in the medium. Next, the cells were fixed with 1 mL, 4 wt% paraformaldehyde in PBS for 15 min. Subsequently, the cells were washed with PBS to remove the excess paraformaldehyde, and incubated with a PBS solution containing DAPI (0.4 μg/mL) for 15 min. Afterwards, the sample was washed and embedded in PBS solution. Fluorescence imaging of the cells was performed with a Leica TCS SP5 microscope. A 40× dry objective lens was used. Excitation of PBA-FSNPs was performed with a laser at the wavelength of 488 nm, and emissions were collected using a wavelength range of 500–535 nm. Also, NHA cells (as the control cell) incubated with PBA-FSNPs, and HeLa cells incubated with FSNPs (as the control probe), both were detected as the same process of HeLa cells incubated with PBA-FSNPs.

3. Results and discussion

In order to develop a simple, sensitive and noninvasive method for labeling SA on the surface of living cancer cells, highly sensitive FSNPs with highly selective PBA tags were prepared by processes depicted in Fig. 1. Herein, the new PBA-FSNPs were prepared through a reverse microemulsion process and a aqueous 'thiol-ene' click reaction, i.e. (1) fluorescence dye molecules of FITC was pre-modified with APTMS, and then polymerized stepwise with TEOS and TEVS to form vinyl-capped FSNPs through reverse microemulsion protocols. Here, the silica matrix of FSNPs acted as a protective shield, which reduces the likelihood of penetration of oxygen and other harmful species that may cause photobleaching of the embedded fluorophores [33–34]; (2) the FSNPs were then covalently conjugated with PBA tags via a thiol-ene click reaction. The UV-induced thiol-ene click reaction was a radical-mediated reaction and benzophenone was used as photoinitiator [30]. The introduced PBA tags on the surface of FSNPs could form stable binding with SA at pH of 7.4 [20,21], and the unique recognizing capability of PBA towards SA and against other sugars would benefit to fabricating a PBA-based FSNPs sensing platform for labeling SA on living cells with good sensitivity and selectivity.

Dye molecules of FITC encapsulated in silica nanoparticles were characterized by UV–vis and fluorescence spectra. Fig. 2A showed UV–vis spectra of silica nanoparticles (SNPs), FITC, and FSNPs in water from 400–700 nm. SNP showed no observable peaks with

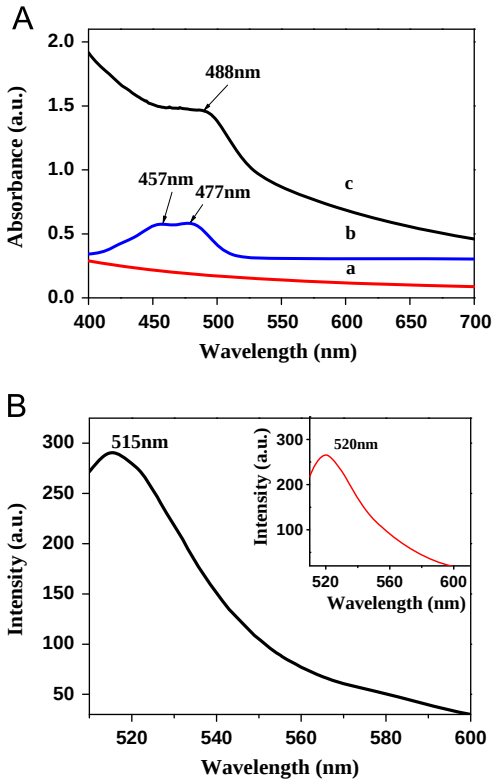

Fig. 2. (A) UV spectra of (a) the SNPs, (b) the FITC and (c) the FSNPs. (B) Fluorescence spectra of PBA-FSNPs and FITC (inset).

the range. FITC showed two characteristic peaks at 457 nm and 477 nm, implying mainly in its anionic form as previously reported [35]. Compared with the FITC, FSNPs showed a characteristic peak at 488 nm and had a little red shift than that of FITC, implying these encapsulated FITCs in FSNPs are mainly in the dianionic form of FITC and might have a little change of molecular structure when FITC is conjugating with APTMS. Importantly, the change in the absorption spectra did not influence the fluorescent property of FSNPs, which is still suitable as an in-vivo imaging probe. Fluorescent spectra of FSNPs showed a characteristic peak at 515 nm with a 5 nm blue shift than that of FITC (Fig. 2B) [36], suggesting that dye molecules of FITC are encapsulated in a silica nanoparticle. It is noticeable that the effective fluorescence intensity of single FSNPs particle is about 366 × brighter than a single dye molecule of FITC. Here, in order to compare the fluorescence intensity of single FSNPs particle with a single FITC, fluorescence spectra of PBA-FSNPs (100 μg/mL) and FITC (75 nM) were measured (as shown in Fig. 2B), and the integral fluorescence intensity of FSNPs and FITC was 10048 au and 10078 au, respectively. Also, in the control experiment, 86.5% fluorescence intensity of FSNPs was preserved after 20 min of UV irradiation, implying the UV-induced thiol-ene click reaction has little effect on the fluorescence of FSNPs. For calculating the fluorescence intensity of single FSNPs particle, the density of the silica nanoparticles material (1.96 g/cm^{-3}) was chosen [37–38], and the average diameter of FSNPs was estimated to be 92.6 ± 9.1 nm (as shown in Fig. 3B,D), and thus the density of FSNPs was about 1.23×10^{11} particles per mL. Similarly, the brightness of a single molecule of FITC dye was also calculated. The integral fluorescence intensity of FITC (75 nM) meant that 4.52×10^{13} dye molecules per mL water was measured. Thus the brightness of single FSNP is equivalent to the brightness of approximately 366 molecules of FITC dye dissolved in water. Moreover, the FSNPs were 7.3 times brighter than that of previously reported fluorescent silica nanoparticles [39]. This high signal amplification is essential to address the growing need for highly sensitive bioassays. Furthermore, as previously reported [40,38], the successful silica coating will expect to improve the photostability and brightness of FITC for living cell analysis.

In order to modify FSNPs with PBA tags, a 'thiol-ene' click reaction was used and the prepared PBA-FSNPs were characterized by TEM, XPS and zeta potential analysis. From the TEM images, it can be concluded both FSNPs and PBA-FSNPs were well-dispersed in water and existed mostly as single particles. The average size of FSNPs was around 85.7 ± 13.4 nm (Fig. 3A, C), while that of PBA-FSNPs increased to 92.6 ± 9.1 nm (Fig. 3B, D). The success of covalent immobilization of PBA on the surface of FSNPs could be ascertained by comparing the XPS spectra of PBA-FSNPs (Fig. 4). PBA-FSNPs exhibited C 1s (284.8 eV), O 1s (533.6 eV), Si 2s (155.2 eV) and N1s (398.8eV) as those of FSNPs. Meanwhile a new peak at 197.6 eV (Fig. 4, the inset) that corresponding to the B 1s region was observed for PBA-FSNPs. Analysis by zeta potential analyzer further confirmed the success of fast and effective surface modification by the thiol-ene click chemistry (Fig. 5). FSNPs were negatively charged with a zeta potential of −39.6 mV (Fig. 5A). This is due to the presence of deprotonated silanol groups (Si–O–) on the silica surface (pKa ~7.0). After the thiol-ene click reaction, the zeta potential of PBA-FSNPs reduced to −23.6 mV (Fig. 5B) due to the high pKa (8–9) of the introducing PBA. Interestingly, the PBA-FSNPs had good dispersibility in water as well as in cell culture medium as FSNPs did, and no clear change of fluorescent intensity in 30 days. The possible reasons are that the decreased negative charges of PBA-FSNPs implies that the FSNPs are partially covalently immobilize with PBA, and the outside silica matrix of PBA-FSNPs can not only preserve good aqueous dispersibility but also work as a protective shield to obtain a stable fluorescence signal.

To confirm the specificity of PBA tags to recognize SA groups on cellular surface, monosaccharide inhibition assay was performed by FCA, where PBA-FSNPs was changed into inhibited PBA-FSNPs by pre-incubating with 5 mM Man, Gal, Glu, or SA for 1 h before incubation with HeLa cells. As shown in Fig. 6A, FCA demonstrated free SA could effectively inhibit the PBA-FSNPs binding on cell surfaces, whereas other monosaccharaides did not show any obvious inhibition in 10 mM pH 7.4 PBS. The reason of the SA-specific inhibition of PBA-FSNPs is SA can exceptionally form stable binding with undissociated PBA on the surface of PBA-FSNPs at physiological pH of 7.4 and other monosaccharides, including Man, Gal and Glu, cannot do. Notably, 5 mM SA could produce 87.6% inhibition of PBA-FSNPs (100 μg/mL) for HeLa cells (as shown in Fig. 6B), but about 200 mM N-acetyl-glucosamine (GLcNAc) would produce the same inhibition of biotinylated wheat germ agglutinin (WGA, a lectin, 50 nM) towards MCF-7 (breast cancer) cells [8]. According to previous reports, the association constant of the PBA-SA at pH 7.4 is 26.6 mM [41] and that of lectin-monosaccharaide was also in the millimolar range [17], and the difference of these affinities between two systems is not obvious. The better affinity of PBA-FSNPs for SA than that of biotinylated WGA for glycan might be ascribed to those advantages of PBA tag rivaling lectins (natural proteins), such as ease of covalent conjugation and long-term stability in tough conditions. Therefore, PBA-FSNPs might be used for imaging SA expressed on living cells with high selectivity.

The selectivity of PBA-FSNPs probe for in-vivo labeling SA was further confirmed by CLSM. HeLa cells were chosen as a model cell because it is reported there are over-expressed SA on their cell membrane. And NHA cells were chosen as the control cell and FSNPs were chosen as the control probe. As shown in Fig. 7, a significant fluorescence signal was observed on the surface of HeLa cells in the presence of PBA-FSNPs (Fig. 7A), suggesting it is the

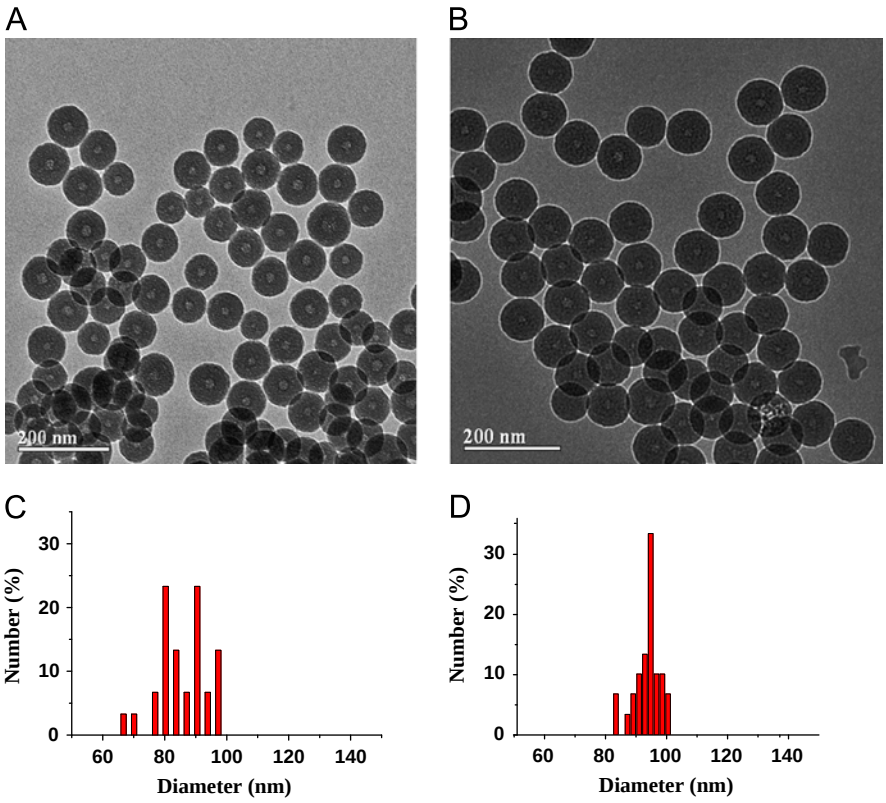

Fig. 3. TEM image of (A) FSNPs and (B) PBA-FSNPs. Diameter distribution of (C) FSNPs and (D) PBA-FSNPs.

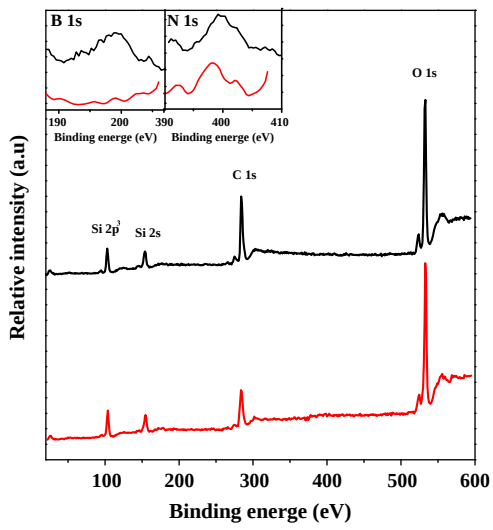

Fig. 4. XPS spectra of FSNPs (red) and PBA-FSNPs (black). Inset in panel: XPS spectra of the N (1s) region and the B (1s) region of FSNP (red) and PBA-FSNPs (black). (For interpretation of the references to color in this figure legend, the reader is referred to the web version of this article.)

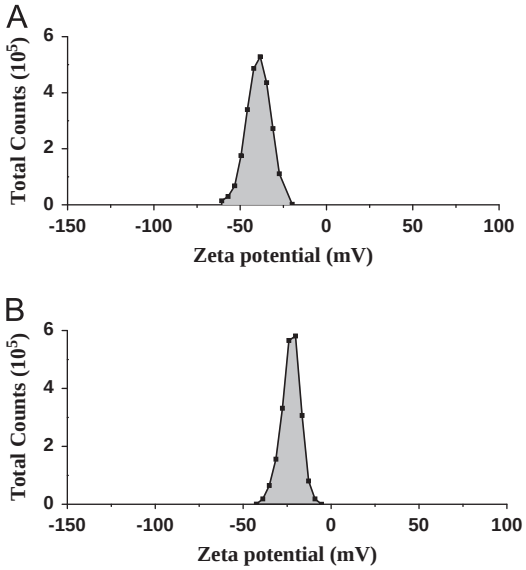

Fig. 5. Zeta potential of (A) FSNPs and (B) PBA-FSNPs.

specific binding between PBA-FSNPs and SA on the surface of HeLa cells, which is consistent with the previous report that SA labeling on the PC12 cell membrane with QDs probes. [22] In contrast, there were no observable fluorescence signal for both the PBA-FSNP-NHA cell system (Fig. 7B) and the FSNP-HeLa cell system (Fig. 7C), implying NHA cell (no over-expressed SA) and FSNPs probe (no PBA tag) both have no strong interaction between the cells and the probes. Furthermore, the line profiles of fluorescence intensity of Fig. 7D–F showed that the PBA-FSNPs probe selectively binds with SA on the surface of these cells. While blue fluorescence of the nuclei were observed for all cell samples (Fig. 7D–F), the intensity of green fluorescence coming from FITC in silica media was only obvious on the outline of HeLa cells with PBA-FSNPs (Fig. 7G), but no for NHA cells with PBA-FSNPs (Fig. 7H) or HeLa cells with FSNPs (Fig. 7I). All these results indicated that PBA-FSNPs exhibits good selectivity and sensitivity as a fluorescence probe for imaging SA on living cells and the promising application. In their application of PBA-FSNPs for cell imaging, the FITC-doped core used as a highly-sensitive “tracer”, and PBA acted as a highly-selective “targeting”.

Biocompatibility is a common characteristic of materials that should be considered when used in biomedicine. For the ultimate

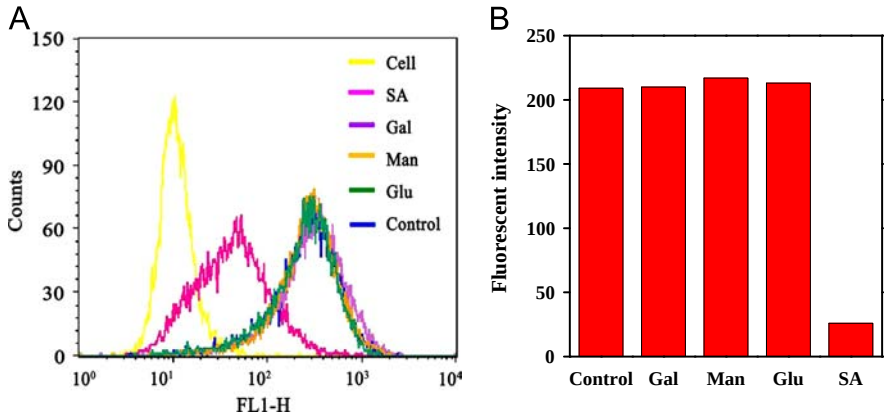

Fig. 6. (A) FCAs of HeLa cells with those inhibited PBA-FSNPs by pre-incubating with different monosaccharaides, including 5 mM Man, Gal, Glu, or SA, respectively, for 1 h before incubation with 1.0×10^6 cells/mL HeLa cells in 10 mM pH 7.4 PBS. Herein, FCAs were performed by counting 10,000 events, and the concentration of PBA-FSNPs was 100 μg/mL. (B) monosaccharide inhibition assay of PBA-FSNPs measured by FCA.

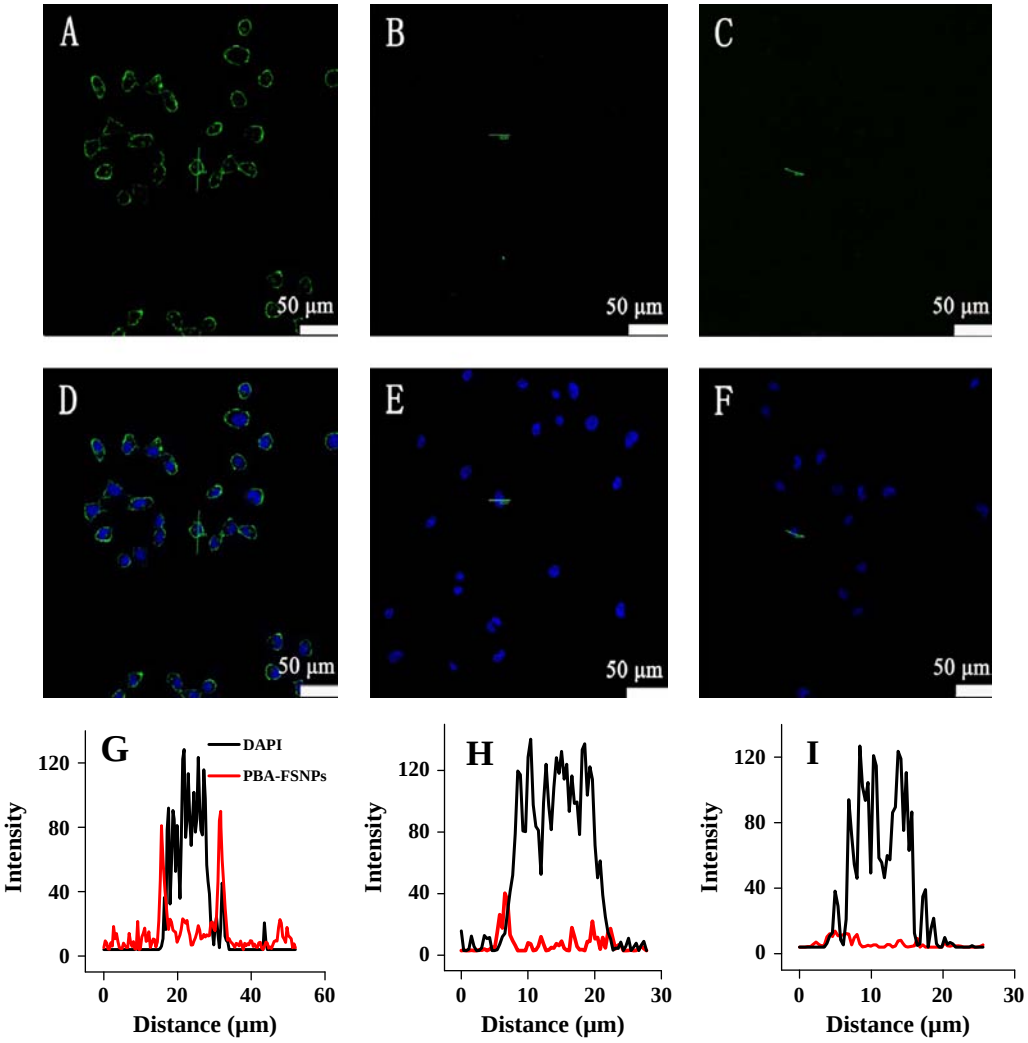

Fig. 7. CLSMs of (A) HeLa cells with PBA-FSNPs, (B) NHA cells (as the control cell) with PBA-FSNPs, and (C) HeLa cells with FSNPs (as the control probe), respectively. The concentrations of PBA-FSNPs and FSNPs were 100 μg/mL. And the cell nuclei were then stained with DAPI (blue). The overlapped fluorescence images of (D) HeLa cells by DAPI and PBA-FSNPs, (E) NHA cells by DAPI and PBA-FSNPs, and (F) HeLa cells by DAPI and FSNPs, and (G–I) their line profiles of fluorescence intensity of fluorescence-immobilized cells. (Scale bar: 50 μm). (For interpretation of the references to color in this figure legend, the reader is referred to the web version of this article.)

use of PBA-FSNPs as specific targeting agent, it is critical to make sure of the lower toxicity of these nanoparticles for living cell and in vivo application. Fig. 8 shows our results of the viability assay labeled with three different concentrations of PBA-FSNPs and FSNPs used in the same manner. The results of MTT assay suggested that the cells maintained over 80% viability after

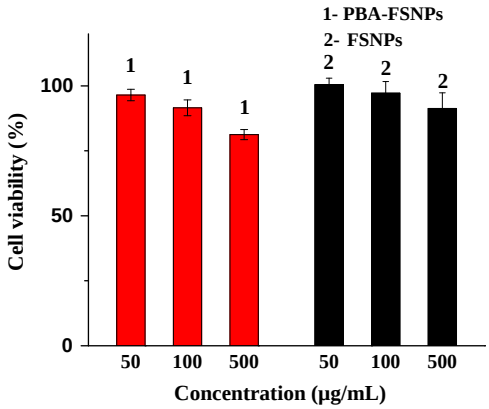

Fig.8. Viability of HeLa cells incubated with different concentrations of PBA-FSNPs (or FSNPs) for 24 h. The percent cell viability is calculated relative to that the cells without the addition of these nanoparticles, which are defined to have a viability of 100%.

incubation with both PBA-FSNPs and FSNPs for 24 h, and obtained 81% viability even at higher concentrations of 500 μg/mL PBA-FSNPs. Thus, it can be concluded that the PBA-FSNPs have good biocompatibility towards HeLa cells.

4. Conclusion

In summary, a facile and efficient synthesis of silica fluorescent probes with PBA tags for imaging of SA on living cells was prepared. Herein, a water-soluble, monodispersed, brighter FSNPs were firstly prepared by a simple one-pot microemulsion method, and then highly selective PBA tags were covalently immobilized on the surface of FSNPs by a thiol-ene click reaction. The successful modification of PBA tags with FSNPs via click reaction was proven by the XPS and zeta potential analysis. The results of FCA and CLSM showed the fluorescent probe of PBA-FSNPs can image SA on the surface of living cells with high sensitivity and selectivity. Also, MTT assays confirmed their good biocompatibility for in-vivo cell imaging. With these favorable properties, the PBA-FSNPs are benefit to fabricate a simple, sensitive and noninvasive method for labeling sialic acid on living cells, and potentially useful for clinical cancer diagnosis and further therapy.

Acknowledgment

This work was supported by National Natural Science Foundation of China (21075021, 21175029 and 20890022) and the Shanghai Leading Academic Discipline Project (B109).

References

[1] M. Fukuda, Cancer Res. 10 (1996) 2237–2244.
[2] R. Raman, S. Raguram, G. Venkataraman, J.C. Paulson, R. Sasisekharan, Nat. Mater. 11 (2005) 817–824.
[3] A. Varki, Trends Mol. Med. 8 (2008) 351–360.
[4] M. Alfonso, A. Diaz, A.M. Hernandez, A. Perez, E. Rodriguez, R. Bitton, R. Perez, A.M. Vazquez, J. Immunol. 5 (2002) 2523–2529.
[5] S.S.S. Wang, D.L. Rymer, T.A. Good, J. Biol. Chem. 45 (2001) 42027–42034.
[6] J.S. Zheng, S.Y. Zheng, Y.B. Zhang, B. Yu, W.J. Zheng, F. Yang, T.F. Chen, Colloids Surf. B: Biointerfaces 1 (2011) 183–187.
[7] L. Krishnamoorthy, L.K. Mahal, Chem. Biol., 9, ACS715–732.
[8] H.H. Jeong, Y.G. Kim, S.C. Jang, H.M. Yi, C.S. Lee, Lab. Chip. 18 (2012) 3290–3295.
[9] K.L. Hsu, K.T. Pilobello, L.K. Mahal, Nat. Chem. Biol. 3 (2006) 153–157.
[10] K.T. Pilcibello, D.E. Slawek, L.K. Mahal, Proc. Natl. Acad. Sci. USA 28 (2007) 11534–11539.
[11] T. Zheng, D. Peelen, L.M. Smith, J. Am. Chem. Soc. 28 (2005) 9982–9983.
[12] L. Ding, W. Cheng, X.J. Wang, S.J. Ding, H.X. Ju, J. Am. Chem. Soc. 23 (2008) 7224.
[13] E. Han, L. Ding, S. Jin, H.X. Ju, Biosens. Bioelectron. 5 (2011) 2500–2505.
[14] D.H. Dube, C.R. Bertozzi, Curr. Opin. Chem. Biol. 5 (2003) 616–625.
[15] J.A. Prescher, C.R. Bertozzi, Cell 5 (2006) 851–854.
[16] J.J. Kohler, Chembiochem 13 (2009) 2147–2150.
[17] H. Lis, N. Sharon, Chem. Rev. 2 (1998) 637–674.
[18] A.B. Iliuk, L.H. Hu, W.A. Tao, Anal. Chem. 12 (2011) 4440–4452.
[19] K.T. Yong, H. Ding, I. Roy, W.C. Law, E.J. Bergey, A. Maitra, P.N. Prasad, ACS Nano 3 (2009) 502–510.
[20] A. Matsumoto, N. Sato, K. Kataoka, Y. Miyahara, J. Am. Chem. Soc. 34 (2009) 12022.
[21] A. Matsumoto, H. Cabral, N. Sato, K. Kataoka, Y. Miyahara, Angew. Chem. Int. Ed. 32 (2010) 5494–5497.
[22] A.P. Liu, S. Peng, J.C. Soo, M. Kuang, P. Chen, H.W. Duan, Anal. Chem. 3 (2011) 1124–1130.
[23] E. Han, L. Ding, H.X. Ju, Anal. Chem. 18 (2011) 7006–7012.
[24] C.W. Lu, Y. Hung, J.K. Hsiao, M. Yao, T.H. Chung, Y.S. Lin, S.H. Wu, S.C. Hsu, H.M. Liu, C.Y. Mou, C.S. Yang, D.M. Huang, Y.C. Chen, Nano Lett. 1 (2007) 149–154.
[25] J.M. Rosenholm, C. Sahlgren, M. Linden, Nanoscale 10 (2010) 1870–1883.
[26] J.L. Vivero-Escoto, I.I. Slowing, B.G. Trewyn, V. Lin, Small 18 (2010) 1952–1967.
[27] H.T. Sun, J.J. Yang, M. Fujii, Y. Sakka, Y.F. Zhu, T. Asahara, N. Shirahata, M. Ii, Z. H. Bai, J.G. Li, H. Gao, Small 2 (2011) 199–203.
[28] R. Fu, G.D. Fu, Polym. Chem. 3 (2011) 465–475.
[29] R.M. Hensarling, V.A. Doughty, J.W. Chan, D.L. Patton, J. Am. Chem. Soc. 41 (2009) 14673.
[30] C. Wang, P.F. Ren, X.J. Huang, J.A. Wu, Z.K. Xu, Chem. Commun. 13 (2011) 3930–3932.
[31] Y. Iwasaki, H. Matsuno, Macromol. Biosci. 11 (2011) 1478–1483.
[32] J.A. Key, C.S. Li, C.W. Cairo, Chem. Biol. 3 (2012) 363–371.
[33] S. Santra, P. Zhang, K.M. Wang, R. Tapec, W.H. Tan, Anal. Chem. 20 (2001) 4988–4993.
[34] S. Santra, K.M. Wang, R. Tapec, W.H. Tan, J. Biomed. Opt 2 (2001) 160–166.
[35] S.P. Dong, M. Roman, J. Am. Chem. Soc. 45 (2007) 13810–13811.
[36] Eun-Bum Cho, Dmytro O. Volkov, Igor Sokolov, Adv. Funct. Mater. 21 (2011) 3129–3135.
[37] L. Wang, K.M. Wang, S. Santra, X.J. Zhao, L.R. Hilliard, J.E. Smith, J. Wu, W.H. Tan, Anal. Chem. 3 (2006) 646–654.
[38] L. Wang, W.H. Tan, Nano Lett. 1 (2006) 84–88.
[39] L.Z. Wang, J.Y. Lei, J.L. Zhang, Chem. Commun. 16 (2009) 2195–2197.
[40] H. Ow, D.R. Larson, M. Srivastava, B.A. Baird, W.W. Webb, U. Wiesner, Nano Lett. 1 (2005) 113–117.
[41] H. Otsuka, E. Uchimura, H. Koshino, T. Okano, K. Kataoka, J. Am. Chem. Soc. 12 (2003) 3493–3502.